



A new approach for a microparts feeding system based on inertial force.

Mickaël Paris, Yassine Haddab, Philippe Lutz

► To cite this version:

Mickaël Paris, Yassine Haddab, Philippe Lutz. A new approach for a microparts feeding system based on inertial force.. 6th International Workshop on Microfactories, IWMF'08., Oct 2008, Evanston, Il., United States. pp.434-439. hal-00331185

HAL Id: hal-00331185

<https://hal.science/hal-00331185>

Submitted on 15 Oct 2008

HAL is a multi-disciplinary open access archive for the deposit and dissemination of scientific research documents, whether they are published or not. The documents may come from teaching and research institutions in France or abroad, or from public or private research centers.

L'archive ouverte pluridisciplinaire **HAL**, est destinée au dépôt et à la diffusion de documents scientifiques de niveau recherche, publiés ou non, émanant des établissements d'enseignement et de recherche français ou étrangers, des laboratoires publics ou privés.

A New Approach for a Microparts Feeding System based on Inertial Force

Mickaël Paris and Yassine Haddab and Philippe Lutz

Automatic Control and Micro-Mechatronic System Department (AS2M)
FEMTO-ST Institute, UMR CNRS 6174 - UFC / ENSMM / UTBM
25000 Besançon, FRANCE
mickael.paris@ens2m.fr, yassine.haddab@femto-st, plutz@femto-st.fr

Abstract—This paper deals with the presentation of a new microparts feeding system based on inertial force and able to move microcomponents with various shapes and sizes. It is a part of our microfactory project, in which different modular elements work together in order to perform assembly tasks [1], [2], [3], [4]. We present the design and the experimental results of this new type of feeder based on the concepts of modularity and flexibility.

Index Terms—Microfactory, Microfeeder, Modularity, Flexibility.

I. INTRODUCTION

Micro-assembly processes require the placement and orientation of small components whose shapes and dimensions can vary widely. Feeding systems are often dedicated to a particular kind of microcomponents, this is the reason why several feeders must be used in a micro-assembly process. Different approaches are used to feed microparts like pneumatic, magnetic and electric feeders [5], [6], [7], [8]. Other systems use the concept of ciliary micromotion [9], or ultrasonic feeder [10]. These micro or meso-systems are conveyors or feeders. Moreover at this scale, dynamics of the microworld makes it difficult to feed very small components because adhesion forces (surface forces) are predominant compared to gravitational forces and the microparts stick to the feeder.

The development of a micropart feeder must take into account the constraints of production which include the criterion of flexibility as well as the intrinsic constraints of micro-objects (i.e roughness, geometry, physicochemical characteristics...) [11] [12]. Located between the storage and the assembly system, feeding systems can have a deep effect on the efficiency of an assembly system [13]. Inside our modular microfactory, the feeder is not dedicated, and take place inside an assembly module. This design is based on the continuity of activities inside the laboratory, like a tool changer [2] and a 2dof (linear-angular) microsystem for example [4] [3]. A module is a square box of $10 \times 10 \times 10 \text{ cm}^3$ which can include different microsystems.

Our approach is based on control mechanical vibrations in order to move the microparts (see Fig. 1). These vibrations allow to break adhesion forces, friction, and drive micro-objects with a high accuracy. The design take into account the criteria of a modular microfactory:

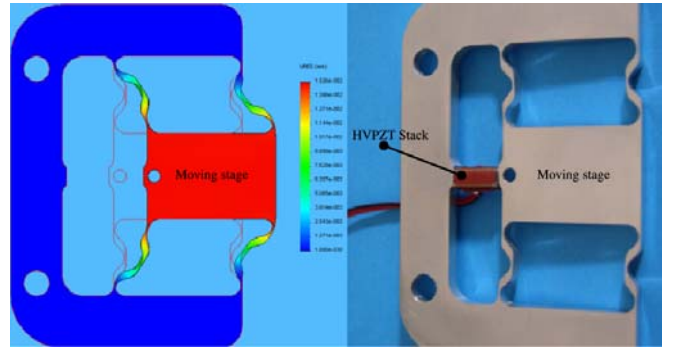


Figure 1. Feeder using inertial force: Feeder by inertial force. (Left) Simulation of the displacement of the table along the X direction, (Right) photography of the feeder and his high voltage piezoelectric actuator.

- 1) save space,
- 2) save energy,
- 3) save cost,
- 4) flexibility and modularity,
- 5) reconfigurable manufacturing system,
- 6) preserving the earth's environment.

II. PRESENTATION OF THE FEEDER

The choice of the inertial force to move micro-objects come from the evaluation of an overview of micromotion systems [11] and from the criteria of a modular microfactory. The concept of a monolithic micromechanical system to move micro-objects is justified by the fact that it is easy to build, and requires low energy. Moreover the control will be easier. We use a high voltage piezoelectric stack actuator to move the moving stage. When the piezoelectric stack is supplied, the moving stage is accelerated. If the acceleration generates a force higher than the friction force and the adhesion forces, the microcomponent will operate a step in the opposite direction of the displacement of the moving stage. The concept of inertial force allows to move different microcomponents with different shapes and sizes. Micro-objects are safe because no prestress is applied on them. The only possible wear is due to friction between the surfaces of the micro-objects and the feeder. Thus feeding by inertial force is suitable for various kinds of microcomponents. We have realized a prototype which as

an effective surface of the moving stage of 27.2 millimeters by 20 millimeters. The feeder has a total width of 80 mm and a total length of 53.96 mm. The flatness of the effective surface is to 1 μm .

III. CHARACTERISATION OF THE FEEDER

This section is dedicated to the characterisation of the transfer function of the feeder. As the acceleration induces displacement of the micro-objects, we must determine the dynamic of the feeder and the influence of the residual vibrations. An interferometer is used to measure the responses of this last one when signals are applied to the piezoelectric stack. The figure 2 shows the setup design for the measures. Since the interferometer is very sensitive to the environmental conditions, the setup was placed under a class 100 vertical laminar flow workstation and on a vibration isolation table. The dynamic behavior of the system has been identified with an Output/Error model under Matlab/Simulink. This estimator gives in our case the best estimation for the model compared to the results given by the ARX and ARMAX estimators. The figure 3 shows the displacements of the moving stage and the result of the evaluation Output/Error estimator when a step is applied to the piezoelectric actuator. The transfer function

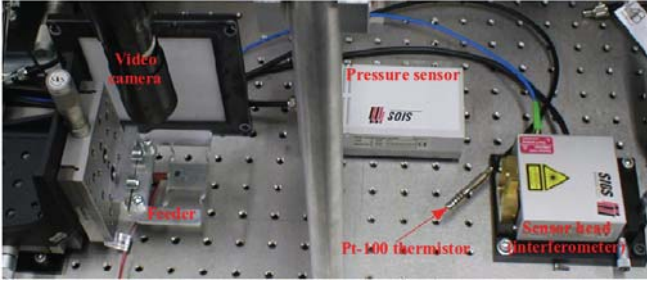


Figure 2. View of the setup.

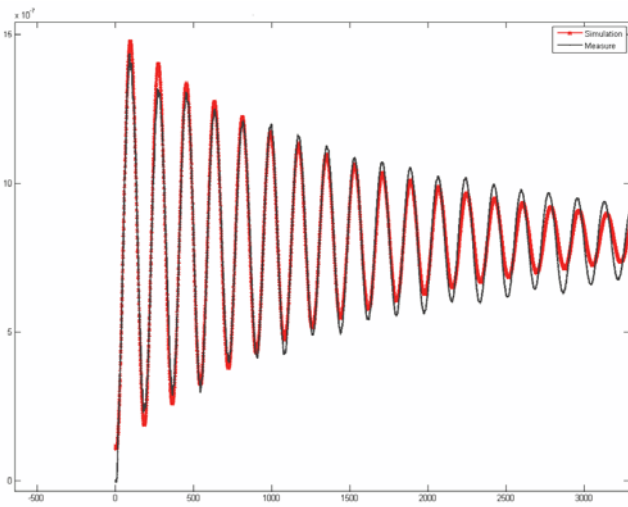


Figure 3. Evaluation of the dynamic of the feeder. Black curve: measurement from the interferometer. Red curve: estimation of the Output Error estimator.

estimated is given by (1):

$$F(s) = \frac{4.935(10^{-6})s + 9.871}{s^2 + 1354s + 1.228(10^9)} \quad (1)$$

The table I resume the different characteristics of the feeder. Since the zero has an influence only in high frequencies

Table I
DYNAMIC CHARACTERISTICS OF THE FEEDER

Characteristics	Value
Damping ratio ζ	0.0193
Natural pulsation w_n	35037 rad.s ⁻¹
Zero	-2.0002 (10 ⁻⁶)
Poles	-0.0677 \pm 3.503i

we can neglect it. Moreover the damping ratio ζ is inferior to 0 so the system oscillates. These oscillations will induce positive and negative accelerations. In these conditions it is not possible to control the step of the micro-objects, so it is necessary to eliminate them in order to move the micro-object and control the step along the right direction.

IV. INPUT SHAPING TECHNIQUE

Input shaping is a feedforward technique for reducing residual vibrations in computer controlled machines. Input shaping is implemented by convolving a sequence of impulses also known as the input shaper, with a desired system command to produce a shaped command that is then used to drive the system [14] (see Fig. 4). Only the estimations of the damping ratio and natural frequency are required to elaborate the time locations and the amplitudes of pulse to reduce residual vibrations. Input shaping can be compared to a Finite Impulse Response (FIR) filtering. The main difference with the traditional filters is that input shapers are not dedicated for a kind of frequencies. Furthermore, as it is explained in [15], shapers are usually designed in the time domain, not the frequency domain. This allows shapers to account for the damping in mechanical systems, whereas, most traditional FIR filters assumes to be undamped frequencies. Input shaping is much more effective for mechanical systems than traditional filters [16], [17], [15]. Moreover, input shaping does not require feedback, so it will not cause stability problems [18]. Figure 5 illustrates the concept of input shaping based on a series of impulses in order to cancel the vibrations coming from a first impulse. A second impulse is applied when the oscillation results from the first impulse is equal to zero with the same magnitude, same frequency and correct phase. The result is like a destructive interference of sinusoidal waves: the total response is set to zero.

The residual vibration that results from a sequence of impulses is described by :

$$V(w_n, \zeta) = e^{\zeta w_n t_n} \sqrt{C(w_n, \zeta)^2 + S(w_n, \zeta)^2}, \quad (2)$$

where,

$$C(w_n, \zeta) = \sum_{i=1}^n A_i e^{\zeta w_n t_i} \cos(w_n t_i), \quad (3)$$

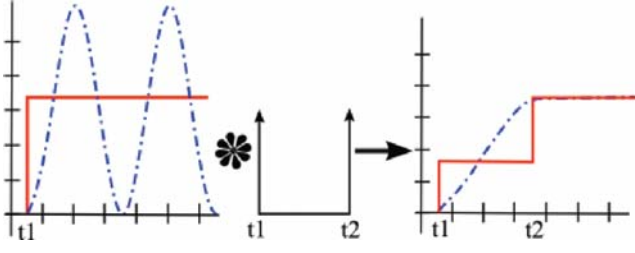


Figure 4. Input Shaping process. The blue curve represents the response of a flexible system and the red curve the input command.

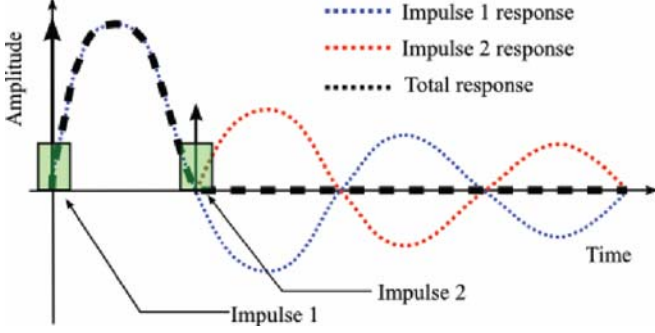


Figure 5. Basic idea of Input Shaping for two impulse response.

$$S(w_n, \zeta) = \sum_{i=1}^n A_i e^{\zeta w_n t_i} \sin(w_d t_i), \quad (4)$$

A_i and t_i are the amplitudes and the time locations of impulses, n is the number of impulses and $w_d = w_n \sqrt{1 - \zeta^2}$. In order to get the residual vibration lead to zero, we must resolve (2) when $V(w_n, \zeta)$ is equaled to zero. To satisfied this condition, the both terms inside the square root of (2) must be set to zero.

$$0 = \sum_{i=1}^n A_i e^{\zeta w_n t_i} \cos(w_d t_i), \quad (5)$$

$$0 = \sum_{i=1}^n A_i e^{\zeta w_n t_i} \sin(w_d t_i). \quad (6)$$

Moreover the sum of the A_i must be equal to 1,

$$\sum_{i=1}^n A_i = 1. \quad (7)$$

Thus for a two impulse response the amplitudes A_1 and A_2 are defined by :

$$A_1 = \frac{1}{1 + K}, \quad (8)$$

$$A_2 = \frac{K}{1 + K}, \quad (9)$$

where,

$$K = e^{(-\zeta \pi) / (\sqrt{1 - \zeta^2})}. \quad (10)$$

To minimize the time delay, the first impulse is placed at $t = 0$ [19], and the second t_2 is calculated from (11):

$$t_2 = \frac{\pi}{w_n \sqrt{1 - \zeta^2}} = \frac{1}{2} \frac{2\pi}{w_n \sqrt{1 - \zeta^2}} = \frac{1}{2} T_d. \quad (11)$$

This second time delay is equaled to the half of the damped period of vibration T_d . The figures 6 and 7 illustrate the effects of input shaping on the moving stage when a step is applied on the piezoelectric stack. The equations for the three impulses are:

$$\begin{bmatrix} A_i \\ t_i \end{bmatrix} = \begin{bmatrix} \frac{1}{(1+K)^2} & \frac{2K}{(1+K)^2} & \frac{K^2}{(1+K)^2} \\ 0 & T_d & 2T_d \end{bmatrix}, \quad (12)$$

and for four impulses:

$$\begin{bmatrix} A_i \\ t_i \end{bmatrix} = \begin{bmatrix} \frac{1}{Den} & \frac{3K}{Den} & \frac{3K^2}{Den} & \frac{K^3}{Den} \\ 0 & T_d & 2T_d & 3T_d \end{bmatrix}, \quad (13)$$

where $Den = 1 + 3K + 3K^2 + K^3$. To get less residual vibrations, a three impulse shaper is conventionally adopted. Generally, the number of impulses is between four and ten. If we get more than two impulses, the system will be less speed but it will be more robust. The main objective is here to control the acceleration of the moving table to generate a sufficient force on the micro-object. At this point, it is not essential to control the final position of the moving table when a control is applied to the piezoelectric actuator. We search to eliminate

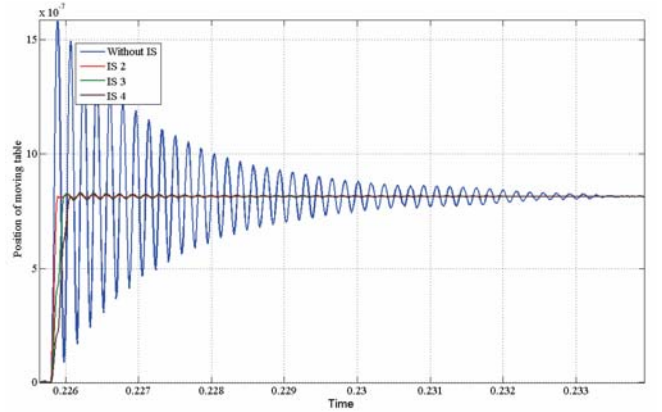


Figure 6. System response for two (red), three (green) and four impulses (brown). The blue curve is the natural response of the moving stage.

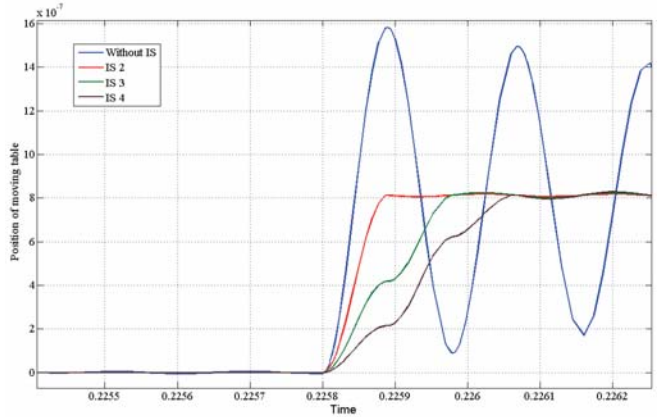


Figure 7. Details of system response for two (red), three (blue) and four impulses (brown).

the residual vibrations and to keep the velocity of the feeder. In these conditions a two impulse input shaper is used.

V. FRICTION AT MICROSCALE

At this scale, the macroscopic friction force models are no longer valid. The laws of Amontons-Coulomb:

- 1) The force of friction is directly proportional to the applied load.
- 2) The force of friction is independent of the nominal area of contact.

don't characterise the frictional phenomenon at the microscopic scale, but only the friction between macroscopic bodies. A surface at the macroscopic scale can appear to be smooth, but if we zoom to the microscopic scale, this surface is rough and is composed of a myriad of asperities. The nominal area of a micro-object is superior to real contact surface which is the sum of all asperities in contact between the surfaces of the micro-object and the feeder. The area of contact is not only influenced by gravity, the adhesion forces can increase or decrease this surface. Because there is no prestress acting on the microcomponents, the normal force is only due to the gravity so the conventional Laws of Amontons-Coulombs could not be used to describe the interaction between the micro-object and the support. The model of friction developed uses the Tabor's theory and the Greenwood-Williamson multi-asperity contact theory [20], [21]. In fifteen, [20] developed the adhesion model of friction between a metallic sphere and a metallic surface, in which, the friction force F_f is proportional to real area of contact A_r :

$$F_f = \tau A_r \quad (14)$$

where τ is the friction stress which is independent of the contact surface. The friction depends on three factors: the real area, the strength of interfacial bonds, and the deformation processes involved when these interfacial bonds are broken during sliding. [21] have extended this model to a surface of contact with multiasperities (see Fig. 8). It is a probabilist model, where rough surfaces are represented by a smooth surface in contact with an equivalent rough surface separated by a distance d . The distribution of the asperities of the equivalent rough surface is defined by a Gaussian distribution $\phi_i(z)$ of asperity heights of the two real surfaces. Moreover, the Greenwood-Williamson model defined the summit of all asperities as spherical, with the same radius R . The area of contact of each asperity can be evaluated by using the Hertz, DMT [22], JKR [23] or Maugis [24] theories. The true area is the sum of each area of asperities in contact of the equivalent rough surface with the perfect smooth surface. The probability of asperities in contact induces a real area of contact defines by:

$$A_r = N \int_d^\infty A(\delta) \phi(z) dz \quad (15)$$

where $A(\delta)$ is the area of a single asperity in contact and N the number of all asperities of the equivalent surface. The total shear force F_r acting on the real surface, is determined

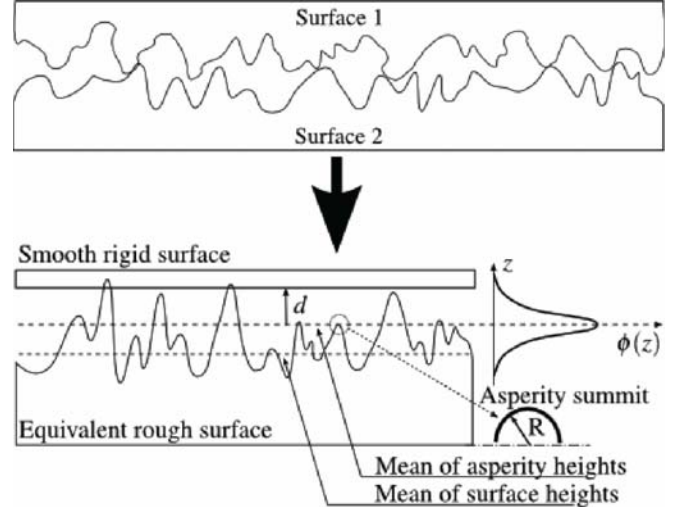


Figure 8. Greenwood-Williamson model of contact mechanics

by integrating the force acting on each single asperity by including (14) in (15):

$$F_r = N \int_d^\infty A(\delta) \tau \phi(z) dz. \quad (16)$$

In order to measure the friction force between the micro-component and the feeder, a setup using an AFM (Atomic Force Microscope) has been used. The AFM's cantilever placed in a vertical position is used to push the microcomponent and the force is measured [12]. Our set-up is used to obtain experimental force curves based on the real-time measurement of the AFM cantilever bending. A force curve is a quasi-static trajectory which correspond to an "approach and retract" cycle between the cantilever and the micro-object (in x direction) (see Fig. 9). When the support and the object are

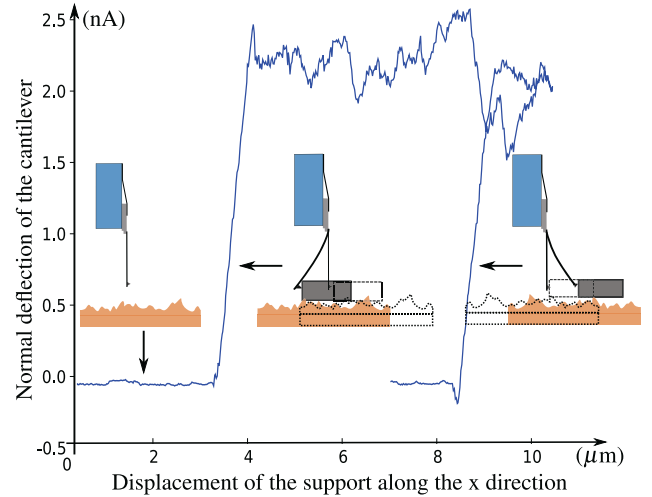


Figure 9. Example of force curve

aligned in y and z directions, the support is moved along the x direction. As soon as the object touches the cantilever, we

observe the normal force which acts on the cantilever, until a maximal value. After that, we observe the sliding of the object on the support. The objective is to find the maximum value of the static friction, for different objects and different supports. The roughness parameters of the equivalent rough surface are evaluated by scanning the surface of the micro-object and the support. The description of these evaluations and the results are described in [12]. For silicon micro-objects placed on a flat support in silicon too, the table II resumes the results obtained [12]. In these experiments, micro-objects

Table II

EVALUATION OF THE INTERFACIAL SHEAR STRESS τ FOR MICRO-OBJECTS PLACED ON A FLAT SUPPORT.

micro-objects	300	200	100	80
Real area $10^{-17}(\text{m}^2)$	4.97	2.21	0.552	0.353
Mean F_r $10^{-6}(\text{N})$	0.94	0.37	0.17	0.08
τ (GPa)	19.03	16.81	25.33	22.91

of $300 \times 300 \times 50 \mu\text{m}^3$, $200 \times 200 \times 50 \mu\text{m}^3$, $100 \times 100 \times 50 \mu\text{m}^3$ and $80 \times 80 \times 50 \mu\text{m}^3$ have been used. We notice that the shear factor is between $16.81 < \tau < 25.33$ (GPa). The obtained result is $22.18 \pm 3.15 \text{ GPa}$, that is equivalent to an uncertainty of 14.2% [12].

VI. THE MODULARITY ASPECT OF THE FEEDER

As we can see, the interaction between the surfaces of the micro-objects and the support influences the friction force. All the parameters which characterise the asperities will get an influence on the value of the friction forces. If the principle by inertial force is estimated as being sufficiently flexible, we can increase his flexibility by developing special surfaces. We consider that the properties of the surfaces of the micro-objects can not be modified. Moreover these surfaces can have different characteristics. As the feeder is not dedicated to a kind of microcomponents, it must be able to move them. So it is possible to place some different supports on the effective area which are dedicated to the characteristics of the micro-objects. Finally these supports will get different roughness. These approach allows to move micro-objects without change the control. Only the parameters of the control will be adapted to the microcomponents. The supports of the feeder become modules in these cases.

The first way is to decrease the nominal area of contact between the surfaces of the micro-objects and the supports. We have realized grooves on the surfaces of supports in order to decrease the real area of contact (see Fig. 10). Two kinds of supports have been built: flat supports and supports with grooves allowing to reduce the surface by half. Let p be the period and h the step height. The nominal area between the micro-object and the support is decreased from 100% to 50%.

The table III show the influence of the grooves on the friction force when an object of $300 \times 300 \times 50 \mu\text{m}^3$ is placed on the flat support and the support with grooves.

An other way is to change material of the support. The area of contact is due to physical and chemical parameters of the bodies in contact as it is described in the Hertz, DMT, JKR and

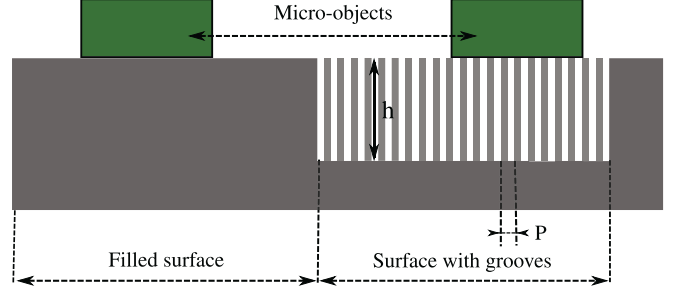


Figure 10. Representation of the supports and the objects used.

Maugis Theories. By the way we can change the interactions and modified the value of the friction force.

It is also possible to operate on the height and the radius of asperities, and so control the friction force too. All these possibilities offer more flexibility and modularity to our feeder by inertial force.

VII. EXPERIMENTS

First experiments on the feeding system have shown the validity of using a vibrating system (Fig. 1) for feeding very small components. The piezoelectric stack is supplied by a sawtooth voltage of 100 Hz and 200 V_{pp} . The obtained displacement for a cuboid of $500 \times 500 \mu\text{m}^2$, is about 3.3 $\mu\text{m}/\text{step}$. Figure 11 illustrates the presents results.

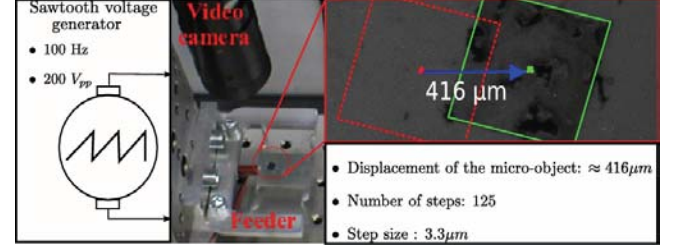


Figure 11. Vibrating experiment.

VIII. CONCLUSIONS

A. Conclusions

In this work we have presented the concept of the feeding by inertial force. The design and development of the feeder has been realized following the criteria of our modular micro-factory. It is a simple monolithic moving table which can move different kinds of microcomponents. This microsystem is designed as a module inside the microfactory. The displacement of the micro-object is realized inertial force.

To control the displacement we have used the Input Shaping technique. After identification of the dynamic behavior of the moving table, the time delays and the amplitudes of impulses have been calculated. We have shown that this control allows to reduce the residual vibrations and then control the acceleration of the feeder.

Table III
EVALUATION OF THE INTERFACIAL SHEAR STRESS τ FOR A 300×300 MICRO-OBJECT

micro-objects	Real area $10^{-17}(\text{m}^2)$ on flat support	Mean F_r $10^{-6}(\text{N})$ on flat support	Mean τ (GPa)	Real area $10^{-17}(\text{m}^2)$ on grooves	Mean F_r $10^{-6}(\text{N})$ on grooves	Mean τ (GPa)
300	4.97	0.94	19.03	3.7833	0.70	18.47

The evaluation of the friction force have been explained too. The setup realized uses an AFM in a non-conventional position.

Experiments have shown the validity of the inertial force approach.

Finally, the modularity aspect of the feeder have been explained.

Future works will study the development of a second moving stage in order to move micro-objects along two direction. Using inertial forces along X and Y directions will allow orientation of micro-objects.

REFERENCES

- [1] E. Descourvières *et al.*, "Towards automatics control for microfactories," in *5th International Conference on INDUSTRIAL AUTOMATION*, 2007.
- [2] C. Clévy *et al.*, "A micromanipulation cell including a tool changer," *Journal of Micromechanics and Microengineering*, pp. S292–S301, 2005.
- [3] M. Rakotondrabe, Y. Haddab, and P. Lutz, "Design, development and experiments of high stroke-precision 2dof (linear-angular) microsystem," *IEEE ICRA*, May 2006.
- [4] —, "Tring module: a high-range and high-precision 2dof microsystem dedicated to a modular micromanipulation station." Besançon France: International Workshop on MicroFactory, December 2006.
- [5] Y. Fukuta *et al.*, "Pneumatic two-dimensional conveyance system for autonomous distributed MEMS," in *The 12th International Conference on Solid State Sensor, Actuator and Microsystems*, Boston, June 8–12 2003, pp. 1019–1022.
- [6] T. Iizuka *et al.*, "A Micro X-Y-theta Conveyor by Superconducting Magnetic Levitation," in *IEEE Symposium on Emerging Technologies and Factory Automation, ETFA'94*, IIS The University of Tokyo, November 6–10 1994, pp. 62–67.
- [7] H. Nakazawa, Y. Watanabe, and O. Morita, "Electromagnetic Micro-Parts Conveyor with Coil-Diode Modules," in *The 10th International Conference on Solid-State Sensors and Actuators, Transducer'99*, vol. 2, no. 1, Sendai, Japan, June 7–10 1999, pp. 1192–1195.
- [8] F. M. Moesner and T. Higuchi, "Contactless manipulation of microparts by electric field traps," in *Proceedings of the SPIE's International Symposium on Microrobotics and Microsystem Fabrication*, vol. 3202, Pittsburgh, October 1997, pp. 168–175.
- [9] J. W. Suh *et al.*, "CMOS Integrated ciliary actuator array as a general-purpose micromanipulation tool for small objects," *Journal of Micro-electromechanical Systems*, vol. 8, no. 4, pp. 483–496, December 1999.
- [10] A. Haake and J. Dual, "Particle positioning by a two- or three-dimensional ultrasound field excited by surface waves," in *WCU*, Paris, 2003.
- [11] M. Paris, C. Perrard, and P. Lutz, "A generic approach for a micropart feeding system," in *Precision Assembly Technologies for Mini and Micro Products*, S. Boston, Ed., vol. 198/2006, 2006, pp. 43–52.
- [12] M. Paris, Y. Haddab, and P. Lutz, "Practical characterisation of the friction force for the positioning and orientation of micro-components," *IEEE IROS*, 2008, in press.
- [13] D. E. Whitney, *Mechanical assembly: their design, manufacture, and role in product development*. New-York, NY: Oxford University Press, 2004.
- [14] W. Singhose, E. Crain, and W. Seering, "Convolved and simultaneous two-mode input shapers," in *IEEE Proceeding of control theory applied*, vol. 144, no. 6, 1997, pp. 515–520.
- [15] W. Singhose and L. Pao, "A comparison of input shaping and time-optimal flexible-body control," *Control Eng. Practice*, 1997.
- [16] N. Singer and W. Seering, "Design and comparison of command shaping methods for controlling residual vibrations," *Proceedings of the IEEE International Conference on Robotics and Automation*, pp. 888–893, 1989.
- [17] N. Singhose, N. Singer, and W. Seering, "Comparison of command shaping methods for reducing residual vibration," *Third European Control Conference*, pp. 1126–1131, 1995.
- [18] B. Rappole, "Minimizing residual vibrations in flexible systems," Master's thesis, Massachusetts Institute of Technology, 1990.
- [19] W. Singhose, "Command generation for flexible systems," Ph.D. dissertation, Massachusetts Institute of Technology, 1997.
- [20] K. N. G. Fuller and D. Tabor, "The effect of surface roughness of the adhesion of elastic solids," in *Proceedings of the Royal Society of London*, ser. A, Mathematical and Physical Sciences, vol. 345, 1975, pp. 327–342.
- [21] J. A. Greenwood and J. B. P. Williamson, "Contact of nominally flat surfaces," in *Proceedings of the Royal Society of London*, ser. A, Mathematical and Physical Sciences, vol. 295, December 1966, pp. 300–319.
- [22] B. V. Derjaguin, V. M. Muller, and Y. P. Toporov, "Effect of contact deformation on the adhesion of particles," *Journal of Colloid and Interface Sciences*, vol. 53, no. 2, pp. 314–326, November 1975.
- [23] K. L. Jonhson, K. Kendall, and A. D. Roberts, "Surface energy and the contact of elastic solids," in *Proceedings of the Royal Society of London*, ser. A, Mathematical and Physical Sciences, vol. 324, 1971, pp. 301–313.
- [24] D. Maugis, "Adhesion of spheres: The jkr-dmt transition using a dugdale model," *Journal of Colloid and Interface Sciences*, vol. 150, no. 1, pp. 243–269, April 1992.